Phase Diagram of Doped Manganates

Daniel P. Arovas[1] and Francisco Guinea[1,2]
[1] *Department of Physics, University of California at San Diego, La Jolla CA 92093*
[2] *Instituto de Ciencia de Materiales, Consejo Superior de Investigaciones Científicas, Cantoblanco, 28049 Madrid, Spain*
(February 1, 2008)

The phase diagram of doped manganate compounds $La_{1-x}A_xMnO_3$ (with divalent A) is studied. We analyze an extension of the double exchange model using the Schwinger boson formalism. Earlier work by de Gennes on the existence of a canted phase is reproduced, although this phase is shown to be unstable towards phase separation in a broad regime of physical interest. We numerically solve the mean field equations for our model and exhibit its phase diagrams.

PACS numbers:

I. INTRODUCTION

Doped manganese oxides show many unusual features, the most striking being the colossal magnetoresistance in the ferromagnetic phase [1–3]. The phase diagram, as function of doping and temperature is far from elucidated. At small dopings, many experiments are interpreted in terms of the phase diagram proposed by de Gennes [4], who studied the so called double exchange model [5] (see below). Some experiments indeed confirm the predictions derived from this approach [6]. Others, however, seem to imply a more complex behavior, including charge ordering [7,8] or coexisting phases [9,10]. In addition, these materials show a metal-insulator transition at low dopings and low temperatures [11].

In the following, we will analyze the phase diagram of these systems using the Schwinger boson representation [12] for the magnetic moments, which are described by the double exchange model. We neglect the role of lattice distortions, which may be important at high dopings, where the Jahn-Teller distortion present in undoped systems disappears [13]. The scheme that we use allows us to obtain a description of the spin waves. In more conventional systems, it has been shown that quantum and thermal fluctuations are adequately described [12,14] in this approach. The method has already been used to study the quasiparticle coherence in the manganese oxides [15]. Finally, the calculations reported here are in general agreement with the work of de Gennes [4] in the in zero temperature, large S limit. The general features of the model are described in the next section. Sections III and IV adapt the Schwinger boson method to the double exchange model. The results for $T = 0$ are presented in section V, where the relation of our work to the original calculation by de Gennes [4] is discussed. Section VI is devoted to finite temperature results. Finally, section VII contains a discussion of experimental results and related thoretical work.

II. MODEL

In materials such as $La_{1-x}A_xMnO_3$ (with A divalent), a fraction x of Mn ions are in $3d^4$ (Mn^{3+}) configurations, with the remaining fraction $1-x$ in $3d^3$ (Mn^{4+}) states. In a cubic crystal field, the Mn $3d$ levels split into a lower t_{2g} triplet and an upper e_g doublet. Intra-atomic ("Hund's rules") couplings overwhelm the crystal field splitting, hence the t_{2g} levels are always triply occupied and form a $S = \frac{3}{2}$ 'core spin'. In Mn^{3+} ions, the e_g orbitals are further split by a static Jahn-Teller (JT) distortion, which, together with the Hund's rules, completely determines both the orbital as well as spin state of the e_g electron. The e_g electrons may be represented by spinless, single-orbital fermions whose hopping is modulated by the overlap of the core spin wavefunctions. If we treat the core spin on site i using the Schwinger representation, $\boldsymbol{S}_i = \frac{1}{2} b^\dagger_{i\alpha} \boldsymbol{\sigma}_{\alpha\beta} b_{i\beta}$ ($\alpha, \beta = \uparrow, \downarrow$, $\sum_\alpha b^\dagger_{i\alpha} b_{i\alpha} = 2S$), then the e_g. electron creation operator $\psi^\dagger_{i\sigma}$ may be factored into a spinless fermion c and the Schwinger boson $b_{i\sigma}$ which supplies the core spin orientation: $\psi^\dagger_{i\sigma} = c^\dagger_i b_{i\sigma}$. The role of the core spin overlap to electron hopping in these materials is widely appreciated (see *e.g.* refs. [4,13,15,16]).

Neighboring core spins are coupled via superexchange through the O $2p$ orbitals [2,17]. For pure $LaMnO_3$ ($x = 0$), the c-axis exchange is antiferromagnetic whilst the exchange between neighboring ions in a plane perpendicular to $\hat{\boldsymbol{c}}$ is ferromagnetic. We have therefore chosen to study the model defined by the Hamiltonian [18]

$$\mathcal{H} = -\tfrac{1}{2} S \sum_{\langle ij \rangle, \sigma} \Big[t_{ij}\, c^\dagger_i c_j\, b_{i\sigma} b^\dagger_{j\sigma} + \text{H.c.} \Big] - \sum_{\langle ij \rangle} J_{ij}\, \boldsymbol{S}_i \cdot \boldsymbol{S}_j$$

for a cubic lattice of Mn ions, where the exchange $J_{ij} = -J_{\rm v} < 0$ along vertical links and $J_{ij} = J_{\rm h} > 0$ along horizontal links. Note that this model is somewhat unrealistic in that the exchange between core spins is fixed independent of the fermion occupancy and hence it cannot reflect the difference between Mn^{3+}-Mn^{3+}, Mn^{3+}-Mn^{4+}, and Mn^{4+}-Mn^{4+} exchange (note that Mn^{4+}-Mn^{4+} exchange, appropriate to pure $CaMnO_3$, is always antiferromagnetic [17]). In addition, we assume a strong static

JT distortion which renders the conduction orbital nondegenerate, whereas in the real materials this distortion vanishes for $x \gtrsim 0.2$. Nonetheless, the model does capture what is perhaps the most important aspect of the interaction between fermions and core spins, namely that ferromagnetic core spin alignment leads to a larger fermion bandwidth and reduced kinetic energy. We aim to apply it in the small x region of the phase diagram, where most of the links are between Mn^{3+} ions. This hopping Hamiltonian itself, in the absence of Heisenberg exchange terms, was considered by Sarker [15], who found a finite temperature transition between a ferromagnetic metal and a spin-disordered state, presumably insulating, in which the fermion band is completely incoherent.

III. MEAN FIELD THEORY

Following Sarker [15], we invoke a Hartree-Fock decoupling of the hopping term:

$$c_i^\dagger c_j \mathcal{F}_{ij} \to -\langle c_i^\dagger c_j\rangle\langle \mathcal{F}_{ij}\rangle + c_i^\dagger c_j \langle \mathcal{F}_{ij}\rangle + \langle c_i^\dagger c_j\rangle \mathcal{F}_{ij} + \text{flucts.}\ ,$$

where $\mathcal{F}_{ij} = b_{j\sigma} b_{i\sigma}^\dagger$ accounts for the overlap of the core spin wave functions. The Heisenberg exchange is treated using the static Schwinger boson mean field theory of ref. [12]. The Hartree-Fock Hamiltonian is then given by

$$\mathcal{H}_{\rm HF} = \mathcal{H}_0 + \mathcal{H}_{\rm hop} + \mathcal{H}_{\rm Bose} + \mathcal{H}_{\rm cond}$$

with

$$\begin{aligned}
\mathcal{H}_0 &= NS^2 J_{\rm v} + 2NS(S+1)J_{\rm h} - 2S\sum_i \Lambda_i \\
&\quad + \frac{2}{J_{\rm h}} \sum_{\langle ij\rangle}^{\rm h} |Q_{\rm h}(ij)|^2 + \frac{2}{J_{\rm v}} \sum_{\langle ij\rangle}^{\rm v} |Q_{\rm v}(ij)|^2 \\
&\quad + \tfrac{1}{2} S \sum_{\langle ij\rangle} \Big[t_{ij}\, \langle c_i^\dagger c_j\rangle\, \langle \mathcal{F}_{ij}\rangle + \text{H.c.}\Big] \\
\mathcal{H}_{\rm hop} &= -\tfrac{1}{2} S \sum_{\langle ij\rangle} \Big[t_{ij}\, c_i^\dagger c_j\, \langle \mathcal{F}_{ij}\rangle + \text{H.c.}\Big] \\
\mathcal{H}_{\rm Bose} &= \sum_{\langle ij\rangle}^{\rm h} [Q_{\rm h}(ij)\, \mathcal{F}_{ij} + \text{H.c.}] + \sum_{\langle ij\rangle}^{\rm v} [Q_{\rm v}(ij)\, \mathcal{A}_{ij} + \text{H.c.}] \\
&\quad + \sum_{i,\sigma} \Lambda_i\, b_{i\sigma}^\dagger b_{i\sigma} - \tfrac{1}{2} S \sum_{\langle ij\rangle} [t_{ij}\, \langle c_i^\dagger c_j\rangle\, \mathcal{F}_{ij} + \text{H.c.}] \\
\mathcal{H}_{\rm cond} &= -\sqrt{N} \sum_{\boldsymbol{k},\sigma} (B_{\boldsymbol{k}\sigma}^* b_{\boldsymbol{k}\sigma} + B_{\boldsymbol{k}\sigma} b_{\boldsymbol{k}\sigma}^\dagger)\ .
\end{aligned}$$

Here, $\sum_{\langle ij\rangle}^{\rm h}$ and $\sum_{\langle ij\rangle}^{\rm v}$ represent sums over horizontal and vertical links, respectively. The Λ_i are Lagrange multipliers which enforce the local constraints $b_{i\alpha}^\dagger b_{i\alpha} = 2S$, $\mathcal{A}_{ij} \equiv (b_{i\uparrow} b_{j\downarrow} - b_{j\uparrow} b_{i\downarrow})$ measures the antiferromagnetic correlation between sites i and j, N is the total number of sites, and $B_{\boldsymbol{k}\sigma}$ is a field which is conjugate to the Schwinger boson condensate order parameter:

$$\Psi_{\boldsymbol{k}\sigma} \equiv \frac{1}{\sqrt{N}} \langle b_{\boldsymbol{k}\sigma}^\dagger\rangle = -\frac{1}{N} \left\langle \frac{\partial F}{\partial B_{\boldsymbol{k}\sigma}} \right\rangle$$

where F is the free energy. We are guided to a simple mean field theory with seven parameters, in which we assume

$$\begin{aligned}
\Lambda &\equiv \Lambda_i \\
\mathcal{F}_{\rm h,v} &\equiv \langle b_{i\sigma}^\dagger b_{j\sigma}\rangle_{\rm h,v} \\
K_{\rm h,v} &\equiv \tfrac{1}{2} t_{\rm h,v} S\, \langle c_i^\dagger c_j\rangle_{\rm h,v} \\
Q_{\rm h} &\equiv Q(ij) \qquad \text{on horizontal links} \\
Q_{\rm v} &\equiv e^{i\boldsymbol{\pi}\cdot\boldsymbol{R}_i}\, Q(ij) \qquad \text{on vertical links}
\end{aligned}$$

are all real constants, where $\boldsymbol{\pi} \equiv (0,0,\pi)$ in units where the lattice constant is unity. Thus, there are seven mean field parameters.

Diagonalizing $\mathcal{H}_{\rm Bose}$, we find

$$\begin{aligned}
\mathcal{H}_{\rm Bose} &= \sum_{\boldsymbol{k},\sigma} E(\boldsymbol{k})\, \beta_{\boldsymbol{k}\sigma}^\dagger \beta_{\boldsymbol{k}\sigma} + \sum_{\boldsymbol{k}} \left(\sqrt{\Lambda_{\boldsymbol{k}}^2 - \Delta_{\boldsymbol{k}}^2} - \Lambda_{\boldsymbol{k}} \right) \qquad (1) \\
&\quad - N \sum_{\boldsymbol{k}} \begin{pmatrix} B_{\boldsymbol{\pi}-\boldsymbol{k}\uparrow}^* & B_{\boldsymbol{k}\downarrow} \end{pmatrix} M^{-1}(\boldsymbol{k}) \begin{pmatrix} B_{\boldsymbol{\pi}-\boldsymbol{k}\uparrow} \\ B_{\boldsymbol{k}\downarrow}^* \end{pmatrix}
\end{aligned}$$

with

$$M(\boldsymbol{k}) = \begin{pmatrix} \Lambda_{\boldsymbol{k}} - \Omega_{\boldsymbol{k}} & \Delta_{\boldsymbol{k}} \\ \Delta_{\boldsymbol{k}} & \Lambda_{\boldsymbol{k}} + \Omega_{\boldsymbol{k}} \end{pmatrix}$$

and

$$\begin{aligned}
\Lambda_{\boldsymbol{k}} &= \Lambda - 2(Q_{\rm h} + K_{\rm h})(\cos k_x + \cos k_y) \\
\Delta_{\boldsymbol{k}} &= -2Q_{\rm v} \cos k_z \\
\Omega_{\boldsymbol{k}} &= -2K_{\rm v} \cos k_z \\
E(\boldsymbol{k}) &\equiv \sqrt{\Lambda_{\boldsymbol{k}}^2 - \Delta_{\boldsymbol{k}}^2} + \Omega_{\boldsymbol{k}}\ .
\end{aligned}$$

When there is a condensate ($T < T_{\rm c}$) the Bose spectrum is gapless, with $\Lambda = \Lambda^*$, where

$$\Lambda^* \equiv 4(Q_{\rm h} + K_{\rm h}) + 2\sqrt{Q_{\rm v}^2 + K_{\rm v}^2}\ .$$

The dispersion then may be compared in the $x \to 0$ limit with the spin wave result

$$E^{\rm sw}(\boldsymbol{k}) = S\sqrt{[J_{\rm v} + J_{\rm h}(2 - \cos k_x - \cos k_y)]^2 - J_{\rm v}^2 \cos^2 k_z}\ ;$$

obtained by expanding about a $(0,0,\pi)$ Néel state (alternating ferromagnetic planes). The basic functional dependence on $\boldsymbol{k}$ is reproduced – this is a good preliminary check on the mean field *Ansatz*.

Note also the particle hole symmetry present in our mean field theory. This guarantees an $x \to 1-x$ symmetry in the phase diagram. As mentioned above, exchange in pure $CaMnO_3$ is different than in pure $LaMnO_3$, due to the presence of the second set of empty e_g states. Hence, this symmetry is an artifact of our model.

In deriving the mean field equations for our model, we must also include the condensate. The relationship between the field $B_{\boldsymbol{k}\sigma}$ and the order parameter $\Psi_{\boldsymbol{k}\sigma}$ is

$$\begin{pmatrix} \Psi_{\boldsymbol{\pi}-\boldsymbol{k}\uparrow} \\ \Psi^*_{\boldsymbol{k}\downarrow} \end{pmatrix} = M^{-1}(\boldsymbol{k}) \begin{pmatrix} B_{\boldsymbol{\pi}-\boldsymbol{k}\uparrow} \\ B^*_{\boldsymbol{k}\downarrow} \end{pmatrix} \ . \tag{2}$$

Differentiating the condensate contribution to the free energy with respect to a generic mean field parameter ξ gives

$$\frac{\partial F_{\rm cond}}{\partial \xi} = N \sum_{\boldsymbol{k}} \begin{pmatrix} \Psi^*_{\boldsymbol{\pi}-\boldsymbol{k}\uparrow} & \Psi_{\boldsymbol{k}\downarrow} \end{pmatrix} \frac{\partial M(\boldsymbol{k})}{\partial \xi} \begin{pmatrix} \Psi_{\boldsymbol{\pi}-\boldsymbol{k}\uparrow} \\ \Psi^*_{\boldsymbol{k}\downarrow} \end{pmatrix} \ .$$

Enacting a global SU(2) rotation $b_{i\sigma} \rightarrow U_{\sigma\sigma'} b_{i\sigma'}$, it is easy to show that the free energy is invariant under such a transformation. This approach to Schwinger boson condensation can also be applied to the cases of the uniform ferro- or antiferromagnet. It has the comforting feature of making the SU(2)-invariance manifest from the outset (compare *e.g.* with ref. [14], in which the condensate always results in a moment in the x-direction).

Proceeding in our analysis, we assume condensation only at $\boldsymbol{k} = 0$ and $\boldsymbol{k} = \pi$. In order that the condensate give no contribution to the free energy, we require that

$$\begin{aligned} \begin{pmatrix} \Psi_{\boldsymbol{\pi}\uparrow} \\ \Psi^*_{0\downarrow} \end{pmatrix} &= -X\, e^{i\gamma} \begin{pmatrix} \cos\frac{1}{2}\vartheta \\ -\sin\frac{1}{2}\vartheta \end{pmatrix} \\ \begin{pmatrix} -\Psi^*_{\boldsymbol{\pi}\downarrow} \\ \Psi_{0\uparrow} \end{pmatrix} &= -Y\, e^{i\delta} \begin{pmatrix} \cos\frac{1}{2}\vartheta \\ -\sin\frac{1}{2}\vartheta \end{pmatrix} \end{aligned} \tag{3}$$

where $\tan\vartheta = Q_{\rm v}/K_{\rm v}$ and X, Y, γ, and δ are at this point arbitrary parameters specifying the direction and magnitude of what is in general a canted $(0, 0, \pi)$ antiferromagnet [4]. Equation 3 also is consistent with the free energy being a convex function of the order parameter $\Psi_{\boldsymbol{k}\sigma}$. The condensate is then spatially varying, with

$$\langle b_{i\sigma} \rangle = \Psi_{0\sigma} + \Psi_{\boldsymbol{\pi}\sigma}\, e^{i\boldsymbol{\pi}\cdot\boldsymbol{R}_i} \ . \tag{4}$$

The condensate contribution to the local magnetization $\langle \boldsymbol{S}_i \rangle$ is easily computed and ϑ is found to be the canting angle.

IV. MEAN FIELD EQUATIONS

We now are in a position to write down the mean field equations. We work in the grand canonical ensemble, introducing a chemical potential μ for the fermions. This introduces an eighth parameter. However, we find that the mean field equations guarantee $Q_{\rm h} = \frac{1}{2} J_{\rm h} \mathcal{F}_{\rm h}$ always, so we are left with the following seven equations:

$$\begin{aligned} 2S &= \int \frac{d^3k}{(2\pi)^3} \frac{\Lambda_{\boldsymbol{k}}}{\sqrt{\Lambda^2_{\boldsymbol{k}} - \Delta^2_{\boldsymbol{k}}}} \,{\rm ctnh}\left(\frac{E(\boldsymbol{k})}{2k_{\rm B}T}\right) + R^2 - 1 \\ \frac{Q_{\rm v}}{J_{\rm v}} &= \int \frac{d^3k}{(2\pi)^3} \frac{Q_{\rm v} \cos^2 k_z}{\sqrt{\Lambda^2_{\boldsymbol{k}} - \Delta^2_{\boldsymbol{k}}}} \,{\rm ctnh}\left(\frac{E(\boldsymbol{k})}{2k_{\rm B}T}\right) + \frac{Q_{\rm v} R^2}{2\sqrt{Q^2_{\rm v} + K^2_{\rm v}}} \\ \mathcal{F}_{\rm h} &= \int \frac{d^3k}{(2\pi)^3} \frac{(\cos k_x + \cos k_y)\, \Lambda_{\boldsymbol{k}}}{2\sqrt{\Lambda^2_{\boldsymbol{k}} - \Delta^2_{\boldsymbol{k}}}} \,{\rm ctnh}\left(\frac{E(\boldsymbol{k})}{2k_{\rm B}T}\right) + R^2 \\ \mathcal{F}_{\rm v} &= 2 \int \frac{d^3k}{(2\pi)^3} \frac{\cos k_z}{\exp\left(\frac{E(\boldsymbol{k})}{k_{\rm B}T}\right) - 1} + \frac{K_{\rm v} R^2}{\sqrt{Q^2_{\rm v} + K^2_{\rm v}}} \\ K_{\rm h} &= \tfrac{1}{4} S t_{\rm h} \int \frac{d^3k}{(2\pi)^3} \frac{\cos k_x + \cos k_y}{\exp\left(\frac{\epsilon(\boldsymbol{k}) - \mu}{k_{\rm B}T}\right) + 1} \\ K_{\rm v} &= \tfrac{1}{2} S t_{\rm v} \int \frac{d^3k}{(2\pi)^3} \frac{\cos k_z}{\exp\left(\frac{\epsilon(\boldsymbol{k}) - \mu}{k_{\rm B}T}\right) + 1} \\ x &= \int \frac{d^3k}{(2\pi)^3} \frac{1}{\exp\left(\frac{\epsilon(\boldsymbol{k}) - \mu}{k_{\rm B}T}\right) + 1} \end{aligned} \tag{5}$$

where $R = \sqrt{X^2 + Y^2}$ is the condensate amplitude, x is the hole concentration, and

$$\epsilon(\boldsymbol{k}) = -S t_{\rm h} \mathcal{F}_{\rm h} (\cos k_x + \cos k_y) - S t_{\rm v} \mathcal{F}_{\rm v} \cos k_z$$

is the fermion dispersion. The integrals are performed over the first Brillouin zone of the cubic lattice. There are seven mean field equations corresponding to seven mean field parameters. The parameters are:

$$\begin{aligned} T < T_{\rm c}: &\quad Q_{\rm v}, \mathcal{F}_{\rm h}, \mathcal{F}_{\rm v}, K_{\rm h}, K_{\rm v}, \mu, R \quad (\Lambda = \Lambda^*) \\ T > T_{\rm c}: &\quad Q_{\rm v}, \mathcal{F}_{\rm h}, \mathcal{F}_{\rm v}, K_{\rm h}, K_{\rm v}, \mu, \Lambda \quad (R = 0) \ . \end{aligned}$$

We have identified several phases which emerge from the mean field theory:

(I) Antiferromagnet (LRO at $\boldsymbol{\pi}$) : $\mathcal{F}_{\rm v}, K_{\rm v} = 0, R \neq 0$
(II) Canted (LRO at 0 and $\boldsymbol{\pi}$) : $Q_{\rm v}, K_{\rm v}, R \neq 0$
(III) Ferromagnet (LRO at 0) : $Q_{\rm v} = 0, R \neq 0$
(IV) 3d Local Magnetic Order : $\mathcal{F}_{\rm v}, \mathcal{F}_{\rm h} \neq 0, R = 0$
(V) 2d Local Magnetic Order : $\mathcal{F}_{\rm v}, R = 0, \mathcal{F}_{\rm h} \neq 0$
(VI) Maximally Disordered : $Q_{\rm v}, \mathcal{F}_{\rm v}, \mathcal{F}_{\rm h}, K_{\rm v}, K_{\rm h}, R = 0$.

The ordered phases I, II, and III were identified by de-Gennes [4]; we have also found evidence of phase separation below $T_{\rm c}$ (see also [19,20]). In what follows we describe our analytical and numerical investigations of the phase diagram.

V. $T = 0$, $S \rightarrow \infty$ LIMIT

Our mean field equations simplify considerably in the limit of zero temperature and $S \rightarrow \infty$. We examine the three ordered ($\Lambda = \Lambda^*$, $R > 0$) phases,

(I) $Q_{\rm v} = S J_{\rm v},\ \mathcal{F}_{\rm h} = 2S,\ \mathcal{F}_{\rm v} = K_{\rm v} = 0$
(II) $Q^2_{\rm v} + K^2_{\rm v} = S^2 J^2_{\rm v},\ \mathcal{F}_{\rm v} = 2K_{\rm v}/J_{\rm v},\ \mathcal{F}_{\rm h} = 2S$
(III) $Q_{\rm v} = 0,\ \mathcal{F}_{\rm v} = \mathcal{F}_{\rm h} = 2S$.

The canted phase II can smoothly interpolate between the $\boldsymbol{\pi}$-antiferromagnet I and the ferromagnet III, with ϑ going from $\frac{1}{2}\pi$ to 0. We start with the canted structure, solving the mean field equation $\mathcal{F}_{\rm v} = 2K_{\rm v}/J_{\rm v}$. We do this in the regime $x \ll 1$ by expanding the fermion dispersion relation

$$\epsilon(\boldsymbol{k}) = \epsilon(0) + St_{\rm v}\mathcal{F}_{\rm v}(1-\cos k_z) + \tfrac{1}{2}St_{\rm h}\mathcal{F}_{\rm h}(k_x^2+k_y^2) + \dots \ ;$$

since $\mathcal{F}_{\rm v} = 0$ is a possible solution, we keep the full c-axis dispersion. We find that the solution is characterized by the dimensionless parameter $r \equiv 8\pi J_{\rm v} t_{\rm h}/t_{\rm v}^2$. For $r > 1$, the only solution has $\mathcal{F}_{\rm v} = K_{\rm v} = 0$, and we have antiferromagnetism at finite doping. However, experiments [22] suggest $J_{\rm v} \approx 0.58\,{\rm meV}$ while spin density functional calculations [23] suggest $t_{\rm v} \approx 44\,{\rm meV}$ (the physical hopping parameter is $S^2 t \approx 100\,{\rm meV}$). This gives $r \approx 0.33$, so the $r > 1$ regime is unphysical for $La_{1-x}A_xMnO_3$. The ground state energy per site is found to be

$$\frac{E_{\rm I}}{NS^2} = -2J_{\rm h} - J_{\rm v} - 4t_{\rm h}x + 2\pi t_{\rm h}x^2 + \dots \tag{6}$$

For $r < 1$, we have a solution with nonzero $\mathcal{F}_{\rm v}$. We find

$$\frac{E_{\rm II}}{NS^2} = -2J_{\rm h} - J_{\rm v} - 4t_{\rm h}x + 2\pi g(r) t_{\rm h}x^2 + \dots \tag{7}$$

$$g(r) = \frac{\pi^2 r - \pi\alpha\sin^2\alpha}{(\sin\alpha - \alpha\cos\alpha)^2}$$

where $\alpha(r) \in [0,\pi]$ is defined implicitly by the equation

$$\alpha - \sin\alpha\cos\alpha = \pi r \ . \tag{8}$$

We obtain $\mathcal{F}_{\rm v} = xt_{\rm v}/J_{\rm v} + \mathcal{O}(x^2)$ in this regime. For $r < \frac{1}{2}$, $g(r) < 0$ and the coefficient of x^2 is negative, indicating phase separation. For $\frac{1}{2} < r < 1$, $g(r) > 0$ and there is a homogeneous, thermodynamically stable canted phase, originally identified by deGennes [4]. Our estimate $r \approx 0.33$ suggests that phase separation is likely.

Within the canted phase, as x increases from 0 to $\frac{1}{2}$, the canting angle decreases from $\vartheta = \frac{1}{2}\pi$ ($\boldsymbol{\pi}$-LRO) to $\vartheta = 0$ (0-LRO). The transition from canted to ferromagnetic order is continuous, occuring at a critical concentration x^* determined by the simultaneous solution of the two equations

$$x^* = \int \frac{d^3k}{(2\pi)^3}\Theta(\mu - \epsilon(\boldsymbol{k}))$$

$$\frac{2J_{\rm v}}{t_{\rm v}} = \int \frac{d^3k}{(2\pi)^3}\cos k_z\,\Theta(\mu - \epsilon(\boldsymbol{k})) \tag{9}$$

in the two variables x^* and μ. For sufficiently large $J_{\rm v}$, ϑ is nonzero even at half-filling and the system remains canted for all x.

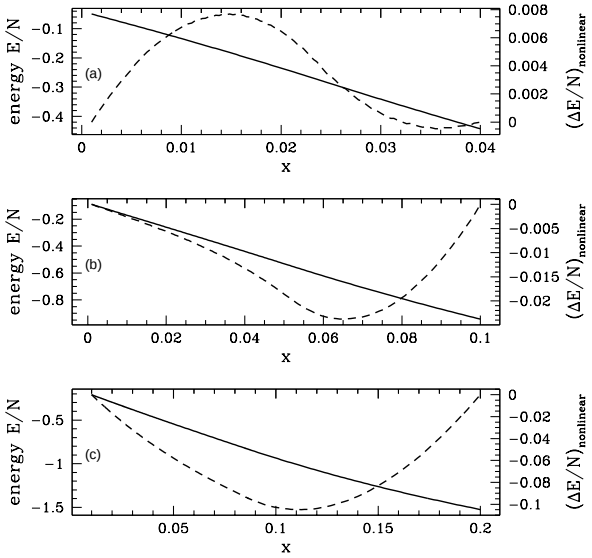

FIG. 1. Energy per site E/N (solid) *versus* concentration x for $J_{\rm v} = J_{\rm h} \equiv J$, $t_{\rm v} = t_{\rm h} \equiv t = 1$ at temperature $T = 0.01\,t$ for three different values of $r = 8\pi J/t$: (a) $r = 0.25$, (b) $r = 0.50$, (c) $r = 0.75$. To ascertain the sign of $\partial^2 E/\partial x^2$, we have subtracted from E/N the linear part; the dashed curve is the remaining contribution. Note that $E(x)$ is convex for small x in (a) and (b), indicative of phase separation.

VI. FINITE T PHASES

To explore the finite temperature phases of our model, we have solved the mean field equations numerically using the `MINPACK` routine `hybrd.f`. (To simplify matters, we assumed $J_{\rm v} = J_{\rm h} \equiv J$ and $t_{\rm v} = t_{\rm h} \equiv t$.) We found that there is often more than one solution to the mean field equations; in such cases we computed the energy of each solution and identified the minimum energy state. To compare with the analytical results of the previous section, we computed the energy *versus* concentration x for three different values of r, all at a temperature well below $T_{\rm c}$ (see figure 1). This verified our prediction of phase separation for $0 < r < \frac{1}{2}$.

In figures 2 and 3 we plot phase diagrams for $J/t = 0.01$ ($r = 0.251$) and $J/t = 0.03$ ($r = 0.754$), respectively. Regions are labeled I through VI corresponding to the six phases discussed above (recall that a condensate is present only in phases I, II, and III). We find that only region III of figure 2 is stable with respect to phase separation. The homogeneous mean field solution yields a convex $F(x,T)$ outside of this region up to temperatures on the order of $T_*(x) \lesssim 0.86\,t$; for $T > T_*$ the free energy is concave in x.

We found a first order line separating phases I and II from the disordered phases. This is so even at $x = 0$ – the mean field theory predicts a first order transition from the $(0,0,\pi)$ Néel state to a magnetically disordered state. This is perhaps a worrisome artifact of the mean field the-

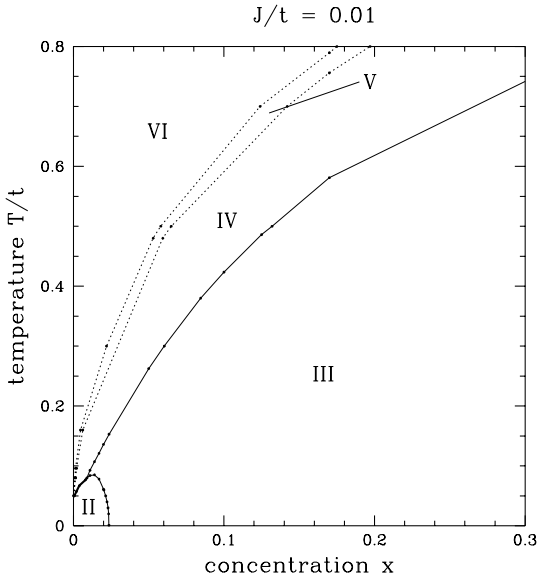

FIG. 2. Phase diagram for $J/t = 0.01$ ($r = 0.251$) obtained from numerical solution of the mean field equations. The dark solid line separating phases II and IV is first order. All other transitions are second order. Dotted lines represent transitions between disordered states. Phase separation occurs outside region III (see text for discussion).

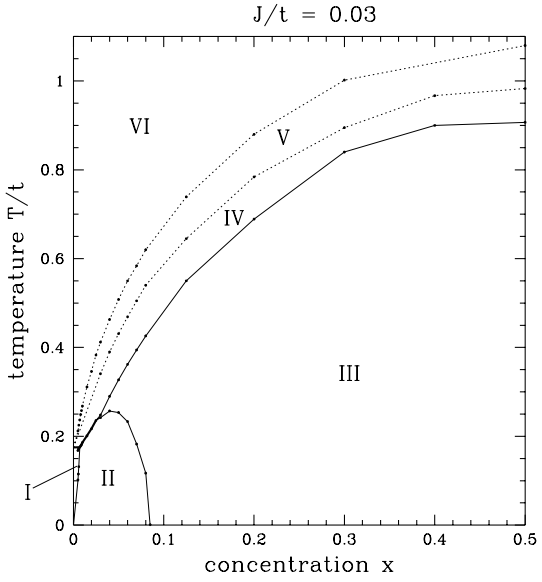

FIG. 3. Phase diagram for $J/t = 0.03$ ($r = 0.754$) obtained from numerical solution of the mean field equations. A small sliver of the $\boldsymbol{\pi}$-ordered phase exists in the lower left corner. The dark solid line separating phases I and IV as well as II and IV is first order. All other transitions are second order. As in figure 2, dotted lines represent transitions between disordered states.

ory. In addition, the transitions between the disordered phases may well become smooth crossovers when fluctuation effects are accounted for. Indeed, application of the Schwinger boson formalism to the Heisenberg model [12] leads to a spurious high temperature mean field transition to a state in which the magnon bandwidth vanishes, analogous to phase VI.

Sarker [15] has discussed the behavior of the electron spectral function and found it to be entirely incoherent when the core spins are disordered. Writing (at finite temperature T)

$$G^{\rm R}_{\alpha\beta}(\boldsymbol{k},t) = -i\langle\{\psi_{\boldsymbol{k}\alpha}(t),\psi^\dagger_{\boldsymbol{k}\beta}(0)\}\rangle\,\Theta(t)$$

$$G^{\rm R}_{\alpha\beta}(\boldsymbol{k},\omega) = \int_{-\infty}^{\infty} d\omega'\,\frac{\rho_{\alpha\beta}(\boldsymbol{k},\omega')}{\omega-\omega'+i0^+}\ ,$$

we find, at the mean field level,

$$\rho_{\alpha\beta}(\boldsymbol{k},\omega) = \int\frac{d^3q}{(2\pi)^3}\left[n_{\alpha\beta}(\boldsymbol{q})+\delta_{\alpha\beta}\,f(\boldsymbol{k}+\boldsymbol{q})\right] \times\delta\left(\omega+E(\boldsymbol{q})-\epsilon(\boldsymbol{k}+\boldsymbol{q})+\mu\right)\ , \quad (10)$$

where $n_{\alpha\beta}(\boldsymbol{q}) = \langle b^\dagger_{\boldsymbol{k}\alpha}\,b_{\boldsymbol{k}\beta}\rangle$ and $f(\boldsymbol{p}) = \langle c^\dagger_{\boldsymbol{p}}\,c_{\boldsymbol{p}}\rangle$ are equilibrium averages. The contribution of the condensate to the spectral density results in well-defined quasiparticle peaks. For instance,

$$\rho^{\rm cond}_{\uparrow\uparrow}(\boldsymbol{k},\omega) = Y^2\sin^2(\vartheta/2)\,\delta(\omega+E(0)-\epsilon(\boldsymbol{k})+\mu) +X^2\cos^2(\vartheta/2)\,\delta(\omega+E(\boldsymbol{\pi})-\epsilon(\boldsymbol{\pi}-\boldsymbol{k})+\mu)\ ,$$

where X, Y, and ϑ describe the amplitude and orientation of the condensate (recall equation 3). The remaining contribution to the spectral function, $\Delta\rho$, is incoherent and spectrally broad [15]. Our calculation allows for condensation both at $\boldsymbol{k}=0$ as well as $\boldsymbol{k}=\boldsymbol{\pi}$, and as expected there are two quasiparticle peaks when translational symmetry is broken (phase I). A detailed study of $\rho(\boldsymbol{k},\omega)$ in the various ordered and disordered phases is pending.

VII. CONCLUSIONS

We have shown that the double exchange model has a variety of possible phase diagrams, controlled by the parameter $r \equiv 8\pi J_{\rm v} t_{\rm h}/t_{\rm v}^2$. For realistic values of r, $0.05 \le r \le 0.2$, we find a phase diagram similar to the one proposed by de Gennes [4], except that the canted phase is replaced by a region of phase separation. In addition, the transition to the paramagnetic phase may be of first order, and the paramagnetic phase itself is anisotropic. For $r > \frac{1}{2}$, we find that the canted phase is stable. The main source of uncertainty in the value of r arises from the lack of a precise determination of the hoppings, which may depend on the composition and details of the lattice structure [3]. Perhaps both situations may be realized experimentally.

Coulomb interactions will prevent charge separation at large scales. The electrostatic energy required to break the system into charged domains of side ℓ goes as $e^2x^2/\epsilon\ell$, where ϵ is the dielectric constant. The magnetic energy

cost to create a domain wall of size ℓ is roughly $J_{\rm v}(\ell/a)^2$, where a is the lattice spacing. Hence, the domain size, ℓ goes as $a^{4/3}(J_{\rm v}\epsilon/e^2x^2)^{1/3}$, which should be on the order of a few lattice constants.

Phase separation in these compounds has previous been discussed phenomenologically in [19], and in [20], in the context of numerical results for the ferromagnetic Kondo lattice in one, two, and infinite dimensions. At large values of the Hund's rule coupling, this model reduces to the double exchange model, plus antiferromagnetic interactions between the core spins. In-plane ferromagnetic interactions do not arise, as they are induced by the second e_g band. Our results, for $T = 0$, are qualitatively in agreement with those reported in [20], provided that one identifies our canted phase with the incommensurate order reported there.

Our calculation reproduces the observed magnon spectrum at zero doping [21], except for a small anisotropy gap. In the canted phase, the long wavelength spin waves behave as $\sqrt{v_\parallel(k_x^2+k_y^2)+v_\perp k_z^2}$. In the phase separated regime, localized ferro- and antiferromagnetic modes are expected, which may have been observed experimentally [22].

A detailed study of transport properties lies beyond the scope of the present calculation. It is interesting to note, however, that, in the presence of phase separation, hopping is suppressed in the out of plane direction in the antiferromagnetic domains. This effect can contribute to make these compounds insulating at low dopings, in agreement with experiments.

VIII. ACKNOWLEDGEMENTS

We are particularly grateful to J. M. D. Coey for educating us on many issues regarding manganates. We also thank A. Millis for useful comments. F. G. acknowledges the hospitality of the University of California at San Diego, where this work was performed.

[1] E. D. Wollan and W. C. Koehler, *Phys. Rev.* **100**, 545 (1955).
[2] See, *e.g.*, J. B. Goodenough, *Magnetism and the Chemical Bond* (Interscience, New York, 1963).
[3] J. M. D. Coey, M. Viret and S. von Molnar, *Adv. in Phys.* (in press, 1997).
[4] P.-G. de Gennes, *Phys. Rev.* **118**, 141 (1960).
[5] C. Zener, *Phys. Rev.* **82**, 403 (1951).
[6] H. Kawano, R. Kajimoto, M. Kubota and H. Yoshizawa, *Phys. Rev. B* **53**, 2202 (1996).
[7] A. Asamitsu, Y. Moritomo, R. Kumai, Y. Tomioka and Y. Tokura, *Phys. Rev. B* **54**, 1716 (1996).
[8] Y. Yamada, O. Hino, S. Nohdo, R. Kanao, T. Inami and S. Katano, *Phys. Rev. Lett.* **77**, 904 (1996).
[9] J. W. Lynn, R. W. Erwin, J. A. Borchers, Q. Huang, A. Santoro, J. L. Peng and Z. Y. Li, *Phys. Rev. Lett.* **76**, 4046 (1996).
[10] M. Viret, H. Glättli, C. Fermon, A. M. de Leon-Guevara and A. Revcolevschi (preprint, 1997).
[11] A. Urushibara, Y. Moritomo, T. Arima, A. Asamitsu, G. Kido and Y. Tokura, *Phys. Rev. B* **51**, 14103 (1995).
[12] D. P. Arovas and A. Auerbach, *Phys. Rev. B* **38**, 316 (1988).
[13] A. J. Millis, P. B. Littlewood, and B. I. Shraiman, *Phys. Rev. Lett.* **74**, 5144 (1995).
[14] S. K. Sarker, C. Jayaprakash, H. R. Krisnamurty and M. Ma, *Phys. Rev. B* **40**, 5028 (1989).
[15] S. K. Sarker, *J. Phys.: Cond. Mat.* **8**, L515 (1996).
[16] C. M. Varma, *Phys. Rev. B* **54**, 7328 (1996).
[17] A. J. Millis, *Phys. Rev. B* **55**, 6405 (1997).
[18] We have scaled the hopping integrals by S^2 in order to allow a large-S analysis of our mean field equations.
[19] E. L. Nagaev, *Usp. Fiz. Nauk* **166**, 833 (1996) [*Physics-Uspekhi* **39**, 781 (1996)]; E. L. Nagaev, *Physica B* **230-232**, 816 (1997).
[20] J. Riera, K. Hallberg and E. Dagotto, *Phys. Rev. Lett.* **79**, 713 (1997); E. Dagotto, S. Yunoki, A. L Malvezzi, A. Moreo, J. Hu, S. Capponi, D. Poilblanc, and N. Furakawa, preprint `cond-mat/9709029`.
[21] F. Moussa, M. Hennion, J. Rodríguez-Carvajal, H. Moudden, L. Pinsard and A. Revcolevschi, *Phys. Rev. B* **54**, 15149 (1996).
[22] M. Hennion, F. Moussa, J. Rodríguez-Carvajal, L. Pinsard and A. Revcolevschi, *Phys. Rev. B* **56**, R497 (1997).
[23] W. E. Pickett and D. J. Singh, *Phys. Rev. B* **53**, 1146 (1996). In the ferromagnetic phase of $La_{2/3}Ca_{1/3}MnO_3$, these authors obtain a total (majority plus minority spins) density of states $\rho(E_{\rm F}) \simeq 0.85/\text{eV}\cdot\text{Mn}$. With $t_{\rm v} = t_{\rm h} \equiv t$, our bandwidth is $W = 12S^2t$, and from $W\rho(E_{\rm F}) \approx 1$ and $S = \frac{3}{2}$ we obtain $t \approx 44\,\text{meV}$.
[24] G. Allodi, R. de Renzi, G. Guidi, F. Licci, and M. W. Pieper, *Phys. Rev. B* **56**, 6036 (1997).
[25] J.-S. Zhou, J. B. Goodenough, A. Asamitsu, and Y. Tokura, *Phys. Rev. Lett.* **79**, 3234 (1997).